

Attribution of 2020 hurricane season extreme rainfall to human-induced climate change

Kevin A. Reed ¹✉, Michael F. Wehner ² & Colin M. Zarzycki³

The 2020 North Atlantic hurricane season was one of the most active on record, causing heavy rains, strong storm surges, and high winds. Human activities continue to increase the amount of greenhouse gases in the atmosphere, resulting in an increase of more than 1 °C in the global average surface temperature in 2020 compared to 1850. This increase in temperature led to increases in sea surface temperature in the North Atlantic basin of 0.4–0.9 °C during the 2020 hurricane season. Here we show that human-induced climate change increased the extreme 3-hourly storm rainfall rates and extreme 3-day accumulated rainfall amounts during the full 2020 hurricane season for observed storms that are at least tropical storm strength (>18 m/s) by 10 and 5%, respectively. When focusing on hurricane strength storms (>33 m/s), extreme 3-hourly rainfall rates and extreme 3-day accumulated rainfall amounts increase by 11 and 8%, respectively.

¹School of Marine and Atmospheric Sciences, Stony Brook University, Stony Brook, NY, USA. ²Applied Mathematics & Computational Research Division, Lawrence Berkeley National Laboratory, Berkeley, CA, USA. ³Department of Meteorology and Atmospheric Science, Pennsylvania State University, State College, PA, USA. ✉email: kevin.reed@stonybrook.edu

Hurricanes are among the most costly and deadly geophysical extremes on Earth. Hurricane damage is caused by extreme wind speeds and flooding due to storm surge and heavy amounts of rainfall over relatively short periods of times. The recent 2020 North Atlantic hurricane season was a clear example of the destruction these storms can inflict on coastlines throughout North America and the Caribbean. The 2020 Hurricane season witnessed a record 30 named storms, 12 of which made landfall in the continental United States¹, resulting in large regions experiencing hurricane rainfall. The total long-term economic costs from these storms are still being quantified, but estimates are over \$40 billion².

Hurricanes are fueled by energy and moisture associated with warm ocean temperatures. Increases in greenhouse gases in the atmosphere due to human emissions have resulted in a detectable increasing trend in global surface land and ocean temperatures over the last century attributable to human activities^{3,4}. Quantifying the impacts of increasing sea surface temperatures (SSTs) on hurricanes, and tropical cyclones globally, remains a scientific challenge, given competing climate effects on other environmental parameters important for storm genesis and development, including wind shear and atmospheric stability⁵. However, a recent assessment by hurricane experts suggests that there has been an increase in intensity and the proportion of the most intense storms, as well as increase in the occurrence of storms resulting in extreme precipitation⁶. This assessment is supported by recent work that has shown evidence of increasing trends in intensity globally⁷.

Beyond studies of decadal trends, attribution frameworks in recent years have been developed to quantify the impact of human-induced warming on hurricane hazards, such as intensity and rainfall, for selected individual devastating storms. The use of hindcast attribution methodologies has demonstrated that human-induced warming has increased rainfall associated recent storms, including Irma and Maria in 2017⁸, Harvey in 2017⁹, Florence in 2018¹⁰, and Dorian in 2019¹¹.

In this work, we apply the hindcast attribution methodology objectively to quantify the climate change impact on extreme rainfall throughout an entire North Atlantic hurricane season for 2020.

Results

Warming fingerprint. Human induced climate change has increased global average surface temperature by over 1 °C as of 2020¹². This global-scale warming has altered the three-dimensional atmospheric states of temperature and moisture (e.g., specific humidity); thermodynamic quantities known to be relevant for hurricane development and formation^{13,14}. The hindcast attribution methodology compares simulations of the actual world to conditional counterfactual simulations of a world without human interference in the climate system¹⁵ and is based on a pseudo-global warming framework¹⁶. Owing to a lack of global-scale preindustrial three-dimensional observational datasets, we construct the initial and boundary conditions defining this counterfactual world by altering observed 2020 conditions by a simulated anthropogenic warming fingerprint from a large climate model ensemble.

The Community Earth System Model (CESM) Large Ensemble¹⁷ is composed of a 1500-year 1850 control simulation and a transient simulation from 1850 onward. Starting in 1920 the initial transient simulation is used to initiate a 40-member ensemble to 2100 with the observed atmospheric composition through 2005 and Representative Concentration Pathway 8.5 boundary conditions afterwards. By averaging over the 40 member ensembles for each month and removing the corresponding 1850 control monthly average (for years 400–1500) we calculate a running estimate of the climate change fingerprint for each calendar month starting in 1920 for all thermodynamic

variables. Note, by using the 1850 control simulation and Representative Concentration Pathway 8.5 forcing, the calculated anthropogenic fingerprint may contain a small solar forcing. Figure 1a shows the temporal evolution of the global average of this fingerprint for surface temperature and demonstrates that the global average temperature anomaly from the preindustrial period is approximately 1 °C in the CESM Large Ensemble for 2020, consistent with observations. A more comprehensive comparison of the CESM Large Ensemble simulated temperature evolution to observations is provided in previous work¹⁷.

2020 hindcast attribution simulations. The 2020 North Atlantic hurricane season was extreme in that it produced 30 named storms. Of these storms, 29 occurred during the official hurricane season between June 1 and November 30, 2020 (Fig. 2). As expected, many of these storms occurred over the warm ocean temperatures of the tropical North Atlantic, where the average SST during the hurricane season was above 27 °C. As shown in Fig. 1b, it is estimated that the human influence on these 2020 SSTs using the CESM Large Ensemble was in the range of 0.4–0.9 °C throughout the majority of the North Atlantic, with an average of about 0.6 °C (Fig. 1a).

To quantify the impact of human-induced climate change on the rainfall associated with the 2020 Hurricane Season we run a series of hindcast simulations for the entire season following the forecast initialization procedure¹⁸ and hindcast attribution methodology¹⁵ with the Community Atmosphere Model (CAM), the atmospheric component of CESM. Week-long ensemble hindcasts are initialized every 3 days starting June 1 through November 30. Hindcasts that are initialized with atmospheric and ocean analyses are referred to as the “actual” ensemble since they are meant to simulate the actual conditions during the 2020 season. An additional ensemble of “counterfactual” hindcasts are also completed in which the surface boundary conditions are adjusted to remove the estimated anthropogenic SST fingerprint (Fig. 1b). The three-dimensional thermodynamic atmospheric variables of temperature and specific humidity are similarly adjusted at initialization using the CESM Large Ensemble and greenhouse gas concentrations are set to 1850 values.

Figure 3(a, b) displays the simulated storm trajectories for all the counterfactual and actual ensembles for the entire 2020 hurricane season when they match an observed storm that is a tropical storm or stronger (winds greater than 18 m/s). As expected, there is spread in the ensembles, but given that 20-member ensembles are initialized every 3 days, there is overlap in the general distribution of tracks for the counterfactual and actual ensembles. The fact that the model is regularly constrained by observed conditions is an advantage of the hindcast attribution approach^{10,11} and allows for a comparison of the simulated storm rainfall.

The ensemble average accumulated rainfall for these storms is also displayed in Fig. 3(c, d). Since the individual ensemble members are 7-day hindcasts, there can be overlap in storm rainfall for events that last longer than 3 days (the time in between initializations). As a result, only 3 days of each ensemble member are included in the accumulated rainfall. Similar to the trajectories, the overall pattern of the simulated accumulated hurricane season rainfall is similar for the counterfactual and actual forecasts. There are subtle differences in certain regions, suggesting different amounts of rainfall for a given storm or slight deviations in ensemble trajectories.

Attribution of hurricane season extreme rainfall. Figure 4 shows the frequency distribution of all (Fig. 4a) 3-hourly storm rainfall rates and (Fig. 4c) 3-day accumulated storm rainfall amounts for the actual and counterfactual ensembles. While

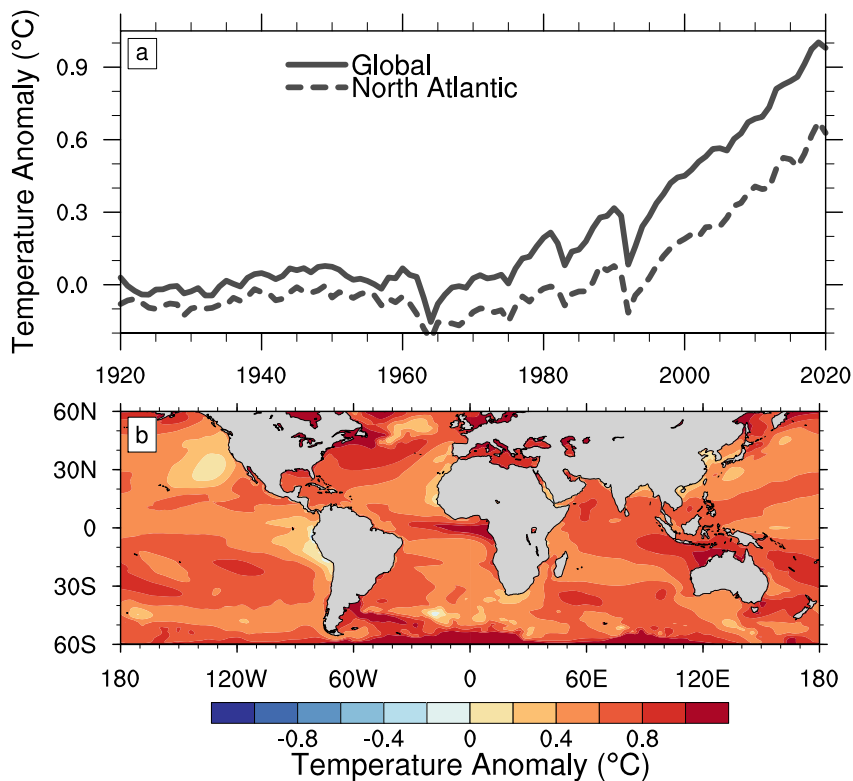


Fig. 1 Global surface temperature change. **a** Evolution of the annual global and North Atlantic (defined to be 0–45°N) average surface temperature anomaly compared to 1850 using the CESM Large Ensemble from 1920 to 2020. **b** Global sea surface temperature anomaly for the 2020 North Atlantic hurricane season (June 1–November 30) relative to 1850 preindustrial period as calculated from the CESM Large Ensemble.

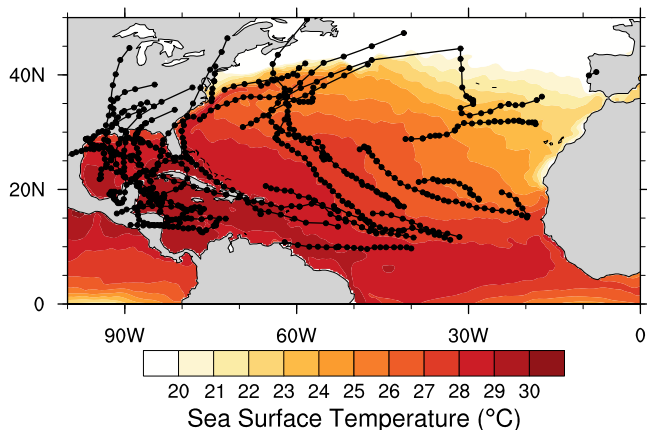


Fig. 2 2020 hurricane tracks and surface temperature. Observed sea surface temperatures (color contours) and hurricane tracks for the 2020 North Atlantic hurricane season (June 1–November 30).

subtle, there are clear differences in the likelihood of both 3-hourly rates and 3-day accumulated amounts between the two ensembles. This is particularly true in the extremes of the distributions (i.e., 99th percentile).

Figure 4b shows the distribution of the 99th percentile storm rainfall rates for each of the individual ensemble members. While there is a large range in simulated 99th percentile rates for each initialization and ensemble due to difference storm intensities at various times in their lifetime, there is a shift toward higher magnitudes in the actual ensemble compared to the counterfactual ensemble. This mean shift from 2.1 to 2.3 in. (~52 to 57 mm) in the 99th percentile of storm precipitation represents an 10.2% increase

due to anthropogenic global warming, with a 95% confidence interval of 5.1 to 15.5%. Performing the same analysis for the 99th percentile accumulated storm rainfall amount (Fig. 4d), reveals an anthropogenic increase in 3-day storm precipitation of 4.8% (95% confidence interval: 0.1 to 9.5%).

If we focus our analysis when observed storms are hurricane strength (surface winds greater than 33 m/s), the 99th percentile hurricane rainfall rate increases from 2.3 to 2.6 in. (~59 to 66 mm), or about 11.3% (95% confidence interval: 6.3 to 16.5%). The change in the 3-day 99th percentile accumulated hurricane rainfall amount 7.8% (95% confidence interval: 4.1 to 11.7%), which is noticeably larger than all storms of tropical storm strength or more.

Discussion

This work quantifies the impact of climate change on rainfall throughout a full hurricane season. Using the CAM hindcast attribution methodology, human-induced climate change increased the extreme (defined to be the 99th percentile) 3-hourly storm rainfall rates and 3-day accumulated storm rainfall amounts during the 2020 hurricane season by 10% and 5%, respectively. This anthropogenic signal is even larger when focusing on storms that are at least hurricane strength, with increases in extreme 3-hourly hurricane rainfall rates and 3-day accumulated hurricane rainfall amounts of 11% and 8%, respectively. This increase in the anthropogenic signal in rainfall from hurricanes compared to rainfall from all tropical storm strength storms is an important finding with direct consequences for coastal communities.

The best estimate of the anthropogenic individual storm rainfall increases, here represented approximately by increases in 3-day accumulations, are consistent with Clausius-Clapeyron (C-C) scaling (~6–7%/C) given the estimated 0.4–0.9 °C anthropogenic warming in the North Atlantic basin. As storm accumulated rainfall is likely limited by available moisture, which in

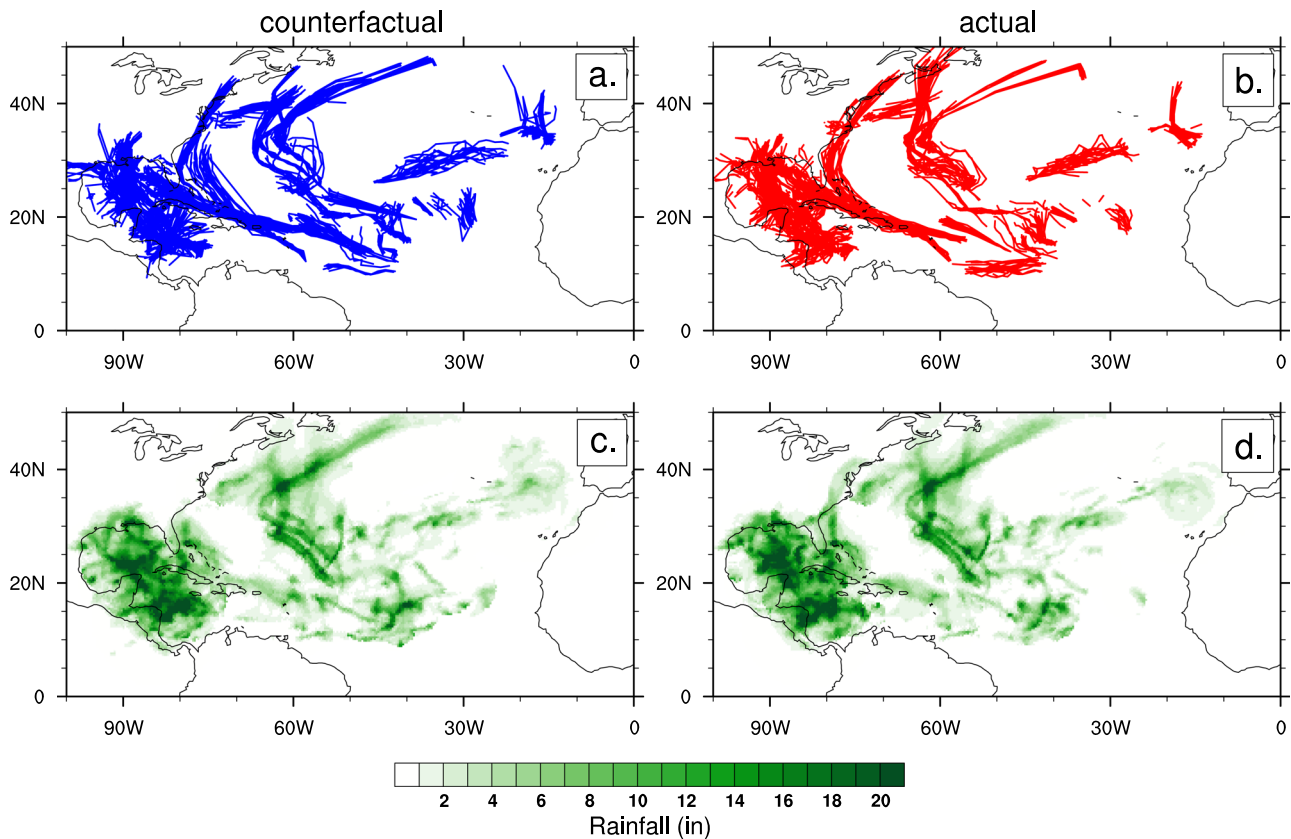


Fig. 3 Actual and counterfactual storm tracks and rainfall. **a, b** Simulated storm tracks that match observed named storms and **c, d** ensemble average accumulated rainfall in inches (in) for the 2020 North Atlantic hurricane season (June 1–November 30) for the **(b, d)** actual and **(a, c)** counterfactual ensembles.

the highly saturated hurricane environment is controlled by C-C scaling, this result is not surprising. However, extreme 3-hourly storm rainfall increases at a rate best estimated at nearly twice C-C scaling, particularly for hurricane strength storms. We note that other work using hindcast attribution methodology at higher model spatial resolutions⁸ found structural changes in precipitation fields with localized total precipitation changes exceeding C-C expectations. As these simulated storms were intensified due to warming, their heaviest precipitating portions exhibited the largest percent rainfall increases. Such dynamical effects on storm structural characteristics could explain the increase in the tail of the hurricane rainfall distribution that we find here, but higher resolution simulations with full three-dimensional output are needed to explore these processes in more detail. Furthermore, while this work indicates that the thermodynamic anthropogenic fingerprint does result in increased rainfall rates and amounts in tropical cyclones, large-scale circulation impacts of climate change on storm frequency and development are not explored in the CAM hindcast attribution methodology.

This work objectively applies the hindcast attribution method to all storms of a given hurricane season, regardless of intensity or coastal impact. Most published work to date has focused, rightly so, on high impact, strong hurricanes with direct damages to coastlines and society. This work agrees with past work that has utilized various attribution frameworks on individual hurricanes to calculate the impact of climate change on storm rainfall to range from 2 to 20% depending on the rainfall metrics^{8–11}. These changes in extreme rainfall associated with the North Atlantic hurricane season are an illustration of the likely climate change impacts on tropical cyclone rainfall in other ocean basins. This work is also consistent with a recent assessment of at least a

“medium-to-high confidence” that an increase the projected future impacts of climate change on global tropical cyclone precipitation rates to be 7% per °C¹⁹, as well as a recent observational finding of a 1.3% global increase in tropical cyclone rainfall rate per year²⁰. Other climate model-based estimates of the imposed pattern and magnitude of warming used to generate the counterfactual ensemble are equally credible but computational constraints preclude examining this source of uncertainty. However as presented here and in earlier studies, precipitation percent changes rather than absolute changes inform the scaling of hurricane precipitation as surface temperature changes. SSTs at both the global and regional scales will continue to increase in the coming decades due to human-induced greenhouse gas emissions. This work suggests that this warming will lead to yet further increases in North Atlantic hurricane season extreme rainfall rates and accumulated amounts. Finally, the application of hindcast attribution frameworks systematically to multiple storms throughout the hurricane season demonstrates the generalizability of such tools for operational climate change attribution applications beyond hurricanes.

Methods

CAM5 hindcast attribution method. This work makes use of the hindcast attribution method with the Community Atmospheric Model, version 5 (CAM)^{10,11,15}. The CAM²¹ hindcasts use a variable resolution configuration with a high-resolution mesh with ~28 k grid spacing over the North Atlantic²². This high-resolution CAM grid has been shown to be sufficient in reproducing the North Atlantic hurricane climatology^{23,24}, as well as storm-related rainfall for individual storms^{10,11} and climatological averages²⁵. 20-member 7-day ensemble hindcasts are initialized every 3 days starting June 1 through November 30 following previous work¹⁸, resulting in 61 initialization times. Hindcasts that are initialized with NOAA atmospheric and ocean analyses from GDAS and OISST are referred to as

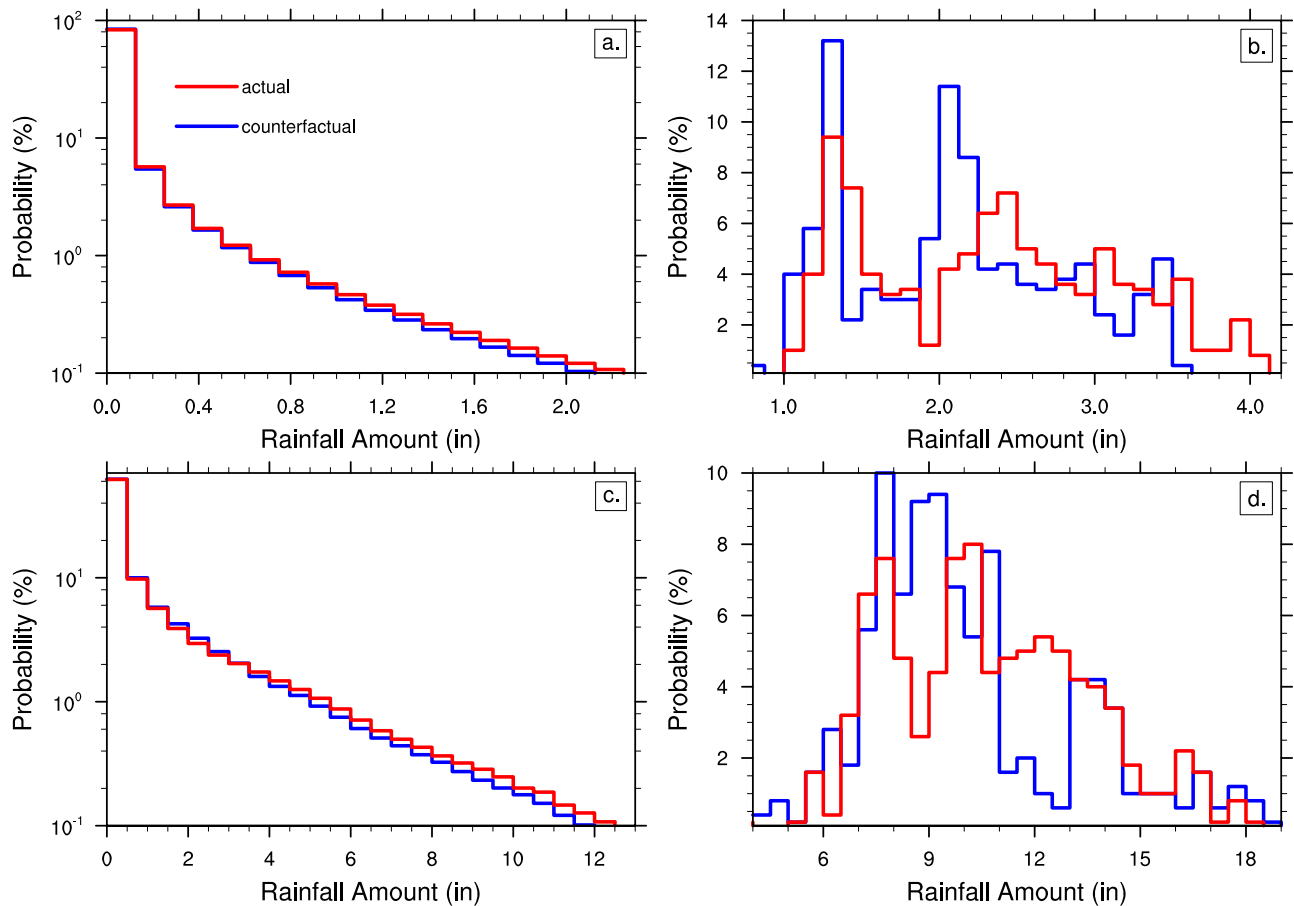


Fig. 4 Changes in storm rainfall. Probability distributions of the **a, b** 3-hourly rainfall rate and **c, d** 3-day rainfall accumulated amounts in inches (in) associated with actual and counterfactual ensemble simulated storms during the 2020 hurricane season for observed storms of at least tropical storm strength. Results are shown for (left) for all rainfall output for all ensembles and (right) the 99th percentile amounts for each individual ensemble and initialization time. The sample size for **b, d** is 500.

the “actual” ensemble since they are meant to simulate the actual conditions during the 2020 season. An additional set of “counterfactual” ensemble hindcasts are also completed in which the seasonal average warming fingerprint for the three-dimensional thermodynamic atmospheric is removed from the initial conditions, the boundary conditions are adjusted to remove the SST fingerprint using the CESM Large Ensemble, and greenhouse gas concentrations are set to 1850 values. Volcanic aerosols and solar forcing are unchanged from the actual ensemble values. Note, that dynamical fields, including the zonal and meridional winds are not adjusted in the counterfactual hindcasts to avoid potential differences in storm trajectories between the ensembles. Both the actual and counterfactual simulations utilize a commonly-used digital filter to remove any hydrostatic imbalance associated with the initial state¹⁸. Finally, the ensemble members are generated using a perturbed parameter approach^{10,11}. In total 1220 individual simulations were completed for both the counterfactual and actual ensembles.

Storm detection and rainfall analysis. To extract precipitation associated only with tropical cyclones for each individual CAM ensemble we use the TempestExtremes software package^{26,27}. TempestExtremes detects candidate cyclones and stitches together trajectories at 3-hourly increments. All analysis for this work only uses simulated storms while the observed storm is tropical storm strength with winds greater than 18 m/s. Furthermore, the simulated storms must initially be within 2 great circle degrees of an observed storm (but this does not have to occur at the initialization time of the ensemble), but after first detection is allowed to diverge by 5 great circle degrees of the observed later in its simulated lifetime. The total number of storms simulated is 1139 for the counterfactual ensemble and 1075 for the actual ensemble. TempestExtremes calculates an outer radius of azimuthally averaged azimuthal wind speed of 8 m/s within which all rainfall is defined to be due to the individual tropical cyclone²⁵. The 99th percentile is then calculated from these storm-only precipitation fields for initializations in which all 20 individual ensemble members simulate an observed storm, which occurs for 25 of the 61 initialization times. All percentage differences and 95% confidence intervals between the actual and counterfactual ensembles are calculated using a bootstrap analysis of 10,000 samples.

Data availability

All raw CAM model output completed for this work is publicly available on the NCAR Globally Accessible Data Environment or is available on Google Drive (CEMSBU) by request due to the large data volume (>2TB). All CESM Large Ensemble output is publicly available via NCAR’s Climate Data Gateway [<https://www.cesm.ucar.edu/projects/community-projects/LENS/data-sets.html>]. All processed CAM storm track files are available on Zenodo [10.5281/zenodo.6046096]. All correspondence should be directed to K.A.R.

Code availability

CAM code is available at www.cesm.ucar.edu and the Betacast (v0.1) code for initializing the hindcast is available on GitHub [<https://github.com/zarzycki/betacast>; <https://doi.org/10.5281/zenodo.6047092>].

Received: 23 June 2021; Accepted: 8 March 2022;

Published online: 12 April 2022

References

- NOAA. *Atlantic Hurricane Season*, accessed: 25th May 2021. Available at: <https://www.nhc.noaa.gov/data/tcr/index.php?season=2020&basin=atl> (2020).
- NOAA National Centers for Environmental Information (NCEI). U.S. Billion-Dollar Weather and Climate Disasters, accessed: 3rd Aug 2021. Available at: <https://www.ncdc.noaa.gov/billions/>.
- IPCC. in *Climate Change 2013: The Physical Science Basis*. Contribution of Working Group I to the Fifth Assessment Report of the Intergovernmental Panel on Climate Change [eds Stocker, T. F. et al.]. (Cambridge University Press, 2013).
- Knutson, T., Kossin, J. P., Mears, C., Perlwitz, J. & Wehner, M. F. *Climate Science Special Report: Fourth National Climate Assessment, Volume I* (eds Wuebbles, D. J. et al.) 114–132 (U.S. Global Change Research Program, 2017).

5. Camargo, S. J. et al. Characteristics of model tropical cyclone climatology and the large-scale environment. *J. Clim.* **33**, 4463–4487 (2020).
6. Knutson, T. et al. Tropical cyclones and climate change assessment: Part I: Detection and attribution. *Bull. Am. Meteorological Soc.* **100**, 1987–2007 (2019).
7. Kossin, J. P., Knapp, K. R., Olander, T. L. & Velden, C. S. Global increase in major tropical cyclone exceedance probability over the past four decades. *Proc. Natl Acad. Sci.* **117**, 11975–11980 (2020).
8. Patricola, C. M. & Wehner, M. F. Anthropogenic influences on major tropical cyclone events. *Nature* **563**, 339–346 (2018).
9. Wang, S. S., Zhao, L., Yoon, J. H., Klotzbach, P. & Gillies, R. R. Quantitative attribution of climate effects on Hurricane Harvey's extreme rainfall in Texas. *Environ. Res. Lett.* **13**, 054014 (2018).
10. Reed, K. A., Stansfield, A. M., Wehner, M. F. & Zarzycki, C. M. Forecasted attribution of the human influence on Hurricane Florence. *Sci. Adv.* **6**, eaaw9253 (2020).
11. Reed, K., Wehner, M. F., Stansfield, A. M. & Zarzycki, C. M. Anthropogenic influence on hurricane Dorian's extreme rainfall. *Bull. Am. Meteorological Soc.* **102**, S9–S15 (2021).
12. Pritchard, H. D. & Turner, J. *State of the Global Climate in 2020*. 56 pp., WMO-No. 1264 (World Meteorological Organization, 2021).
13. Gray, W. M. *Hurricanes: Their Formation, Structure and Likely Role in the Tropical Circulation. Meteorology over the Tropical Oceans*. 155–218 (Royal Meteorological Society, James Glaisher House, 1979).
14. Camargo, S. J., Tippett, M. K., Sobel, A. H., Vecchi, G. A. & Zhao, M. Testing the performance of tropical cyclone genesis indices in future climates using the HIRAM model. *J. Clim.* **27**, 9171–9196 (2014).
15. Wehner, M. F., Zarzycki, C. M. & Patricola, C. Estimating the human influence on tropical cyclone intensity as the climate changes. *Hurric. Clim. Change*, (Springer, 2019) **4**, 235–260 (2019).
16. Schär, C., Frei, C., Lüthi, D. & Davies, H. C. Surrogate climate-change scenarios for regional climate models. *Geophys. Res. Lett.* **23**, 669–672 (1996).
17. Kay, J. E. et al. The Community Earth System Model (CESM) large ensemble project: a community resource for studying climate change in the presence of internal climate variability. *Bull. Am. Meteorological Soc.* **96**, 1333–1349 (2015).
18. Zarzycki, C. M. & Jablonowski, C. Experimental tropical cyclone forecasts using a variable-resolution global model. *Monthly Weather Rev.* **143**, 4012–4037 (2015).
19. Knutson, T. et al. Tropical cyclones and climate change assessment: Part II: Projected response to anthropogenic warming. *Bull. Am. Meteorological Soc.* **101**, E303–E322. 20 (2020).
20. Guzman, O. & Jiang, H. Global increase in tropical cyclone rain rate. *Nature Communications*, **12**, 5344 (2021).
21. Neale, R. B. et al. Description of the NCAR community atmosphere model (CAM 5.0). *NCAR Tech. Note NCAR/TN-486+ STR 1*, 1–12 (2010).
22. Zarzycki, C. M. et al. Aquaplanet experiments using CAM's variable-resolution dynamical core. *J. Clim.* **27**, 5481–5503 (2014).
23. Wehner, M. F. et al. The effect of horizontal resolution on simulation quality in the Community Atmospheric Model, CAM5.1. *J. Adv. Model. Earth Syst.* **6**, 980–997 (2014).
24. Zarzycki, C. M. & Jablonowski, C. A multidecadal simulation of Atlantic tropical cyclones using a variable-resolution global atmospheric general circulation model. *J. Adv. Model. Earth Syst.* **6**, 805–828 (2014).
25. Stansfield, A. M., Reed, K. A., Zarzycki, C. M., Ullrich, P. A. & Chavas, D. R. Assessing tropical cyclones' contribution to precipitation over the eastern united states and sensitivity to the variable-resolution domain extent. *J. Hydrometeor.* **21**, 1425–1445 (2020).
26. Ullrich, P. A. & Zarzycki, C. M. TempestExtremes: a framework for scale-insensitive pointwise feature tracking on unstructured grids. *Geoscientific Model Dev.* **10**, 1069–1090 (2017).
27. Ullrich, P. A. et al. TempestExtremes v2.1: a community framework for feature detection, tracking and analysis in large datasets. *Geoscientific Model Dev.* **14**, 5023–5048 (2021).

Acknowledgements

This work was partially supported by the Stony Brook Foundation's Minghua Zhang Early Career Faculty Innovation Fund, the Department of Energy (DOE) Office of Science award number DE-SC0016605 "A Framework for Improving Analysis and Modeling of Earth System and Intersectoral Dynamics at Regional Scales," and at LBNL by the Director, DOE Office of Science, DOE Office of Biological and Environmental Research under Contract No. DE340AC02-05CH11231. We would like to acknowledge high-performance computing support from Cheyenne (doi:10.5065/D6RX99HX) provided by NCAR's Computational and Information Systems Laboratory, sponsored by the NSF.

Author contributions

K.A.R. completed the model simulations, directed the analysis, and drafted the manuscript. M.F.W. helped to interpret the results and C.M.Z. aided in the setup of the hindcast model framework. Both M.F.W. and C.M.Z. provided critical feedback that helped shape the final manuscript.

Competing interests

The authors declare no competing interests.

Additional information

Correspondence and requests for materials should be addressed to Kevin A. Reed.

Peer review information *Nature Communications* thanks the anonymous reviewer(s) for their contribution to the peer review of this work.

Reprints and permission information is available at <http://www.nature.com/reprints>

Publisher's note Springer Nature remains neutral with regard to jurisdictional claims in published maps and institutional affiliations.



Open Access This article is licensed under a Creative Commons Attribution 4.0 International License, which permits use, sharing, adaptation, distribution and reproduction in any medium or format, as long as you give appropriate credit to the original author(s) and the source, provide a link to the Creative Commons license, and indicate if changes were made. The images or other third party material in this article are included in the article's Creative Commons license, unless indicated otherwise in a credit line to the material. If material is not included in the article's Creative Commons license and your intended use is not permitted by statutory regulation or exceeds the permitted use, you will need to obtain permission directly from the copyright holder. To view a copy of this license, visit <http://creativecommons.org/licenses/by/4.0/>.

© The Author(s) 2022, corrected publication 2022